Journal of Applied Electrochemistry **34**: 563–576, 2004.

Review in Applied Electrochemistry. Number 54

Recent developments in polymer electrolyte fuel cell electrodes

E. ANTOLINI
Scuola di Scienza dei Materiali, via 25 aprile 22, 16016 Cogoleto, Genoa, Italy
(Correspondence, e-mail: ermantol@libero.it)

Received 27 June 2003; accepted in revised form 15 December 2003

Key words: diffusion layer, electrocatalysts, gas diffusion electrodes, polymer electrolyte fuel cells (PEFC)

Abstract

Since the 1980s there has been a significant lowering of the platinum loading of polymer electrolyte fuel cell electrodes from about 4–10 mg cm^{-2} (platinum black) to about 0.4 mg cm^{-2} or even less (carbon supported platinum), by the introduction of ionomer (liquid Nafion®) impregnated gas diffusion electrodes, extending the three-dimensional reaction zone. From the 1990s to the present studies have been carried out to decrease the loss of performance during cell operation due both to the presence of liquid water causing flooding of the catalyst layer and mass transport limitations and to the poisoning of platinum by the use of reformed fuels. This review deals with the developments in electrode configuration going from dual layer to three layer electrodes. The preparation methods, the characteristics and the optimal composition of both diffusion and reactive layers of these electrodes are described. The improvement in the performance of both CO tolerant anodes and cathodes with enhanced oxygen reduction by Pt alloying is also discussed.

1. Introduction

Polymer electrolyte fuel cells (PEFCs) are a promising future option for traction power. Portable and residential applications are also attracting attention. Compared with other fuel cell systems they have the advantage of high power densities at relatively low operating temperatures (~80 °C); they are also small and lightweight. A PEFC consists of an anode, to which hydrogen fuel is supplied, a cathode to which oxygen (or air) is supplied, and a perfluorosulfonic acid (Nafion®) electrolyte membrane that permits the flow of protons from anode to cathode. Costamagna and Srinivasan [1, 2] reviewed the 'quantum jumps' in PEFC science and technology from the 1960s to the year 2000. According to the authors, the 'quantum jumps' which enabled the rapid advances in the technology were the transition from polystyrene sulfonic acid to perfluorosulfonic acid membranes, a 10 to 100-fold reduction in the platinum loading in the electrode, and the optimization of electrode and membrane/electrode assemblies. Since the 1980s there has been a significant lowering of the platinum loading of electrodes from about 4–10 mg cm^{-2} (platinum black) to about 0.4 mg cm^{-2} or even less (carbon supported platinum), by the introduction of ionomer (liquid Nafion®) impregnated gas diffusion electrodes [3–5], extending the three-dimensional reaction zone. From the 1990s to the present studies have been carried out with the aim of increasing the performance and the lifetime of low Pt loading electrodes by the optimization of water management.

Water transport in fuel cells is not well understood. An approach to the problem of water transport via the mechanism of surface diffusion was adopted by Bevers et al. [6]. Another approach via the hydraulic pressure and the potential gradient was suggested by Bernardi and Verbrugge [7]. The prevailing literature opinion is that gas is transported to the reaction sites via hydrophobic pores whereas water is transported out of the electrode through the hydrophilic pores. Based on these assumptions with increasing water loading pores are closed for gas transport by the water. In the cathode diffusion medium the product water flows towards the channel through gas-phase diffusion or liquid-phase motion. The humidification of oxygen gas makes it difficult for diffusion, therefore, liquid water becomes present in the diffusion medium. At high current densities, the liquid flow rate increases due to increased condensation, and when the channel is at the local vapour saturation condition, liquid water flows out of the diffusion medium and surface droplets are formed. On these bases, the importance of the presence of a diffusion layer between the support and the catalyst layer is widely recognized [8–10]. The diffusion layer plays a decisive role in cell water management as well as in the humidification of the membrane electrolyte. Both

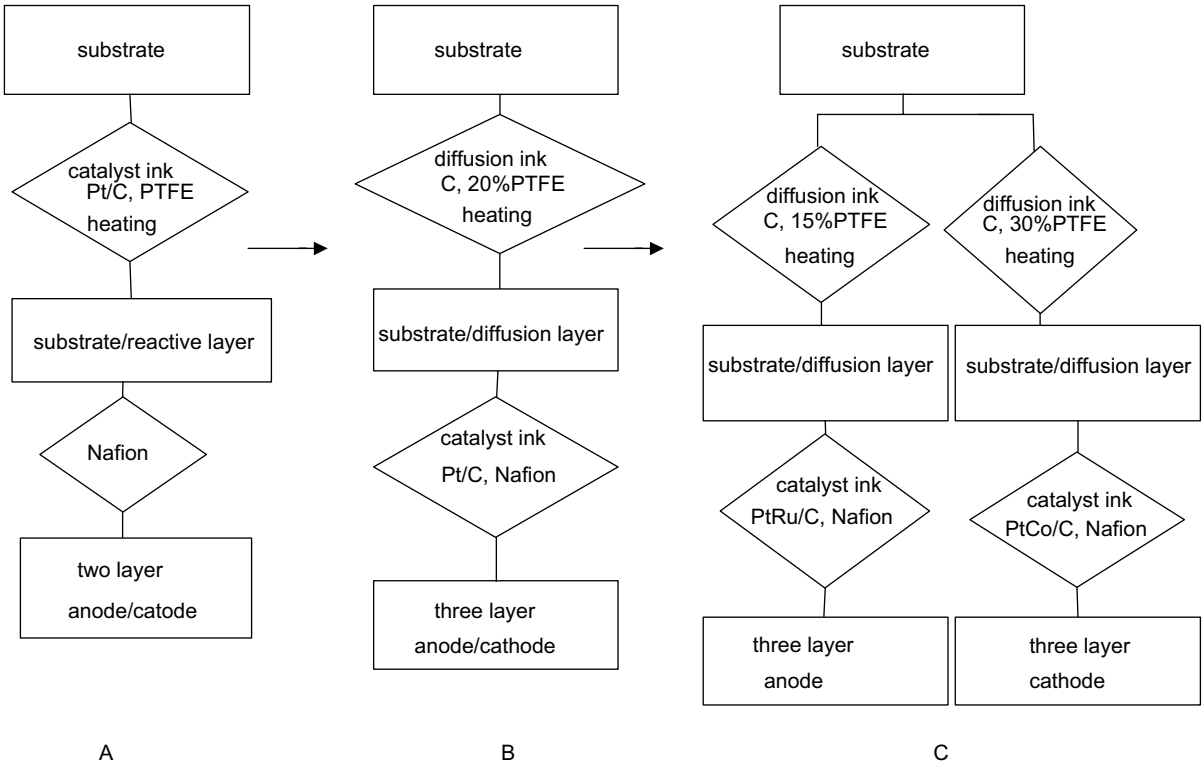

Fig. 1. Evolution of the preparation method of PEFC electrodes from two-layer (A) to three-layer (B) structure, and of anode and cathodes from the same (B) to different (C) composition of both diffusion and catalyst layer.

diffusion and reactive layers consist of a substrate with a certain thickness, tortuosity and porosity. Bevers et al. [6], in a theoretical model, showed that the cell performance and the limiting current depend on porosity and pore size of both diffusion and reaction layers of the electrodes.

An improvement in diffusion layer characteristics, minimizing the mass transport problems, is particularly useful for the cathode, mainly working at elevate pressures in H_2/air operation. As can be seen in the flow chart of the preparation of PEFC electrodes shown in Figure 1, the development of these electrodes in recent years went from a two layer (A) to a three layer (B) electrode, using the same chemical composition for both anode and cathode. The next step was to design anodes and cathodes with different chemical composition of both the diffusion layer and the catalyst layer (C). Better water management in the cell was achieved using anode and cathode with different content of the hydrophobic agent. Another remarkable improvement in long time cell performance in the last decade was made by using Pt alloys to enhance both the tolerance to reformed fuels and the oxygen reduction reaction (ORR). The evolution of the active layer of both anodes and cathode is shown in Figure 2. The present work analyses the advances in PEFC electrodes in the last decade with particular attention to the optimization of both diffusion and reaction layers. The use of carbon supported Pt alloy electrocatalysts in the preparation of CO-tolerant anodes, as well as in the fabrication of cathodes with improved kinetics of the oxygen reduction reaction, is also reviewed.

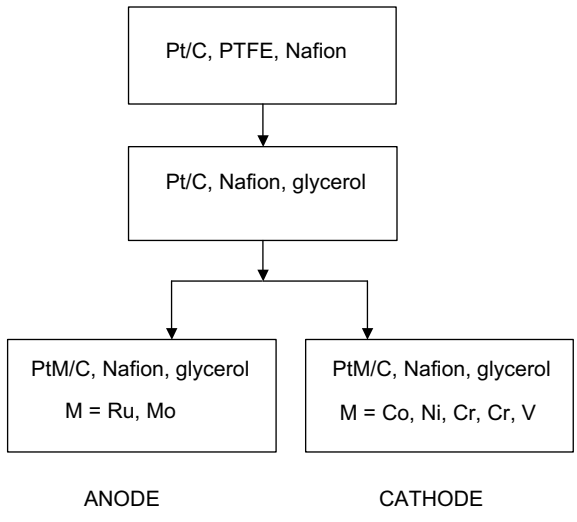

Fig. 2. Evolution of anode and cathode catalyst layer composition.

2. Electrode configuration and preparation

Essentially there are three kinds of PEFC electrodes:

(a) carbon paper + catalyst layer, used particularly in the early 1990s. The standard dual layer structure is composed of a porous catalyst layer and a hydrophobic support layer.

Table 1. Characteristics of some carbon papers used as support in polymer electrolyte fuel cell electrodes [11]

Carbon paper	Thickness /mm	Porosity /%	Bulk density /g cm^{-3}
Toray TGPH 090	0.30	77	0.45
Kureha E-715	0.35	60–80	0.35–0.40
Spectracarb 2050A-1040	0.25	60–90	0.40

(b) carbon paper + diffusion layer + catalyst layer. Three layer electrodes consist of a porous backing layer, a diffusion layer formed by carbon particles and polytetrafluoroethylene (PTFE) and a catalyst layer formed by carbon supported platinum (Pt/C) and ionomer.

(c) carbon cloth + two diffusion sublayers (one on the catalyst side and the other on the gas side of the support) + catalyst layer.

2.1. *Type (a) and (b) electrodes: the effect of carbon paper*

The characteristics of some carbon paper substrates used in PEFCs are shown in Table 1. The effect of the kind of substrate on the performance of polymer electrolyte membrane fuel cells using electrodes with and without a diffusion layer is shown in Figure 3 [11]. As can be seen, in H_2/O_2 operation the best cell performance was obtained using Kureha E-715 as electrode substrate both for the cells with type (a) and type (b) electrodes. From the results reported in Figure 1 and the data shown in Table 1, it can be deduced that the performance of the electrodes depends on the thickness of the carbon paper, but it could depend also on the morphological characteristics of the supports. In recent work Qi and Kaufman [10] found that the presence of a diffusion layer reduces the difference among different carbon paper types made by different manufacturers. In this case, the carbon paper seems to function merely as a support that provides the mechanical strength for the layer.

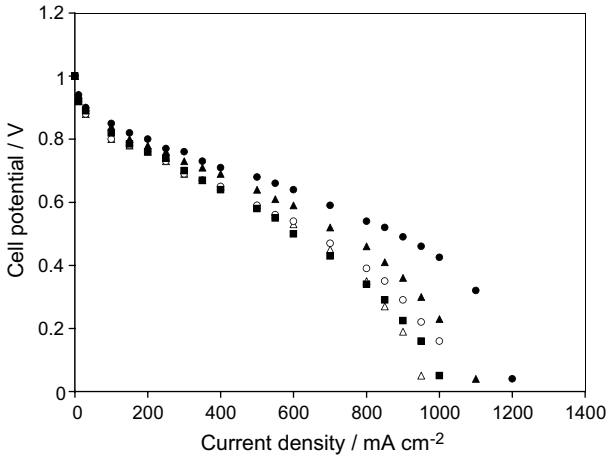

Fig. 3. Cell performance of type (a) and type (b) electrodes with different support. Cell temperature 70 °C, in H_2/O_2 (2.5/3 bar) [11]. (○) substrate Kureha/30% FEP; (△) substrate Toray/30% FEP; (●) substrate Kureha/0%FEP; (▲) substrate Toray/0% FEP; (■) substrate Spectracarb/0% FEP. Empty symbols: type (a) electrodes, catalyst layer with 40 wt % PTFE, Nafion® loading 0.9 mg cm^{-2}, Pt loading 0.5 mg cm^{-2}. Full symbols: type (b) electrodes, diffusion layer with carbon loading 2 mg cm^{-2} and 40 wt % PTFE, and catalyst layer with Nafion® loading 0.2 mg cm^{-2} and Pt loading 0.1 mg cm^{-2}.

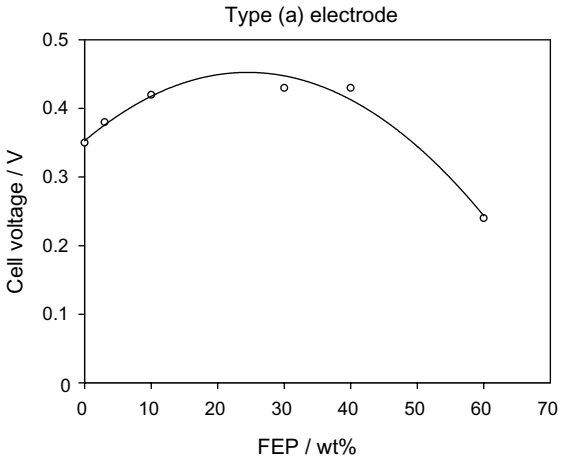

Fig. 4. Dependence of cell voltage on fluoroethylenepropylene (FEP) content of the carbon paper [13].

2.2. *Type (a) electrode*

The substrate is wet-proofed with fluoroethylenepropylene (FEP) or PTFE. The loading of the hydrophobic material in the substrate influences the mass transport properties of the electrode, and thus the cell activity. Figure 4 shows the effect of FEP loading of the carbon paper on the cell voltage at a current density of 200 mA cm^{-2}. A maximum in the cell performance is found at about 30 wt% FEP [12, 13]. This behaviour is the sum of the gas diffusion and the ionic resistance effects. Both of these, which are related to water transport phenomena, are strongly dependent on the FEP loading. The reactive layer usually consists of carbon supported Pt or Pt alloy electrocatalyst, Nafion® and PTFE for wet-proofing and as a binder. Generally, a homogeneous suspension of the catalyst and PTFE is applied directly on the wet-proofed carbon paper. Uchida et al. [14], instead, prepared the catalyst layer by mixing the catalyst with acetylene black carbon (weight ratio 70:30), treated in advance to have 30 wt% PTFE. After deposition of the reactive layer without Nafion® on the substrate, the electrode is dried in air at 70–120 °C, then thermally treated at 280 °C to remove the dispersant agent present in PTFE, and finally sintered at 350 °C.

Few studies on the effect of PTFE amount on the morphology of the Pt/C–PTFE layer have been carried out [15, 16]. Watanabe et al. [15] showed that there is a bimodal pore size distribution in the porous mass of

platinized carbon bonded with PTFE, with the boundary between the two pore classes at about 0.1 μm. The hydrophobic fluorine resin is located principally in the large pores, which are filled by gas and, as a consequence, are not reactive sites. Then, the hydrophobicity is related to porosity (not a free parameter) as the PTFE coating can only be included with a sacrifice in the pore volume. The PTFE amount in the catalyst layer is a determining parameter for the wettability of the electrode [17]. Nam and Kaviany [18] studied the formation–distribution of condensed water in PEFC diffusion medium, and its tendency to reduce the local effective mass diffusivity and to influence cell performance. They found that the larger porosity is better for both the reduction of water saturation and increase in limiting current density. As a consequence, increasing the hydrophobicity by adding more PTFE coating material is questionable. According to Cheng et al. [19], the melted PTFE disperses in the catalyst layer very uniformly. They observed no large PTFE clumps or wide net-like structures. Aricò et al. [20] found that the optimum PTFE content in the catalyst layer is 30 wt%, to attain the minimum charge transfer resistance. If the PTFE is too low, flooding of part of the reactive layer occurs. An excess of polymer causes a decrease in both the ionic conductivity and the electrochemically active surface area. Uchida et al. [21] prepared the reactive layer of a dual electrode without PTFE, placing the Nafion® in the catalyst ink: in this case, the ionomer also serves as the binder of the reactive layer. In this method the Nafion® solution is converted into a colloid by adding an organic solvent. This procedure resulted in a good network of Nafion® to achieve uniformity of the ionomer on the catalyst particles. In the presence of PTFE, the Nafion® can be introduced in the catalyst layer only by impregnation, after thermal treatment of the electrode. Nafion® may be applied by brushing, spraying or by floating/dipping the electrode in a Nafion® solution. The disadvantage of Nafion® impregnation is the difficulty of controlling the amount of Nafion® applied, and the impossibility of achieving a homogeneous distribution of the ionomer in the reactive layer.

Following Nafion® impregnation by an immersion method, transmission electron micrographs revealed the presence of some thick Nafion® layers and clumps in the catalyst layer [19]. Lee et al. [22], using a thin film agglomerate model, assumed a rapid increase in the film thickness with Nafion® loading in the pores of the carbon of the catalyst layer followed by an equilibrium of about 80 nm thickness at a Nafion® loading of 1.9 mg cm^{-2}. Further additions caused deeper penetration of this Nafion® film into the reactive layer, increasing the diffusional pathway for the reactant gases. Poltarzewski et al. [23] investigated the effect of Nafion® loading in dual layer electrodes on their electrochemical activity. The impregnation of the electrolyte in the reactive layer was made by floating the electrodes on a Nafion® solution. They found that the

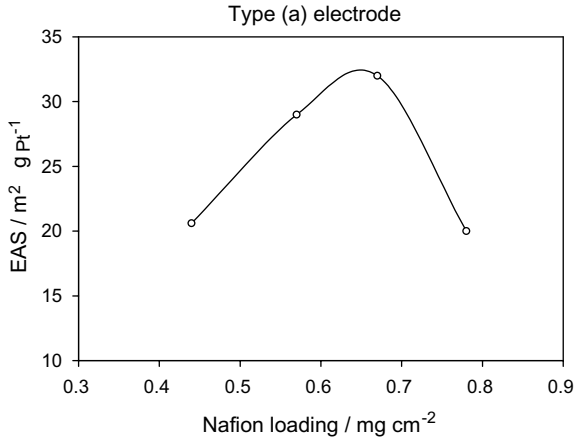

Fig. 5. Electrochemically active surface area against Nafion® content in the catalyst layer of type (a) electrodes [24].

Nafion® loading mostly influences the ionic resistance of the catalyst layer. From 0.8 to 1.0 mg Nafion® cm^{-2} a maximum in electrochemical activity was observed. In this range the ionic resistance of the electrode reaches its lowest value. This behaviour was explained according to the previously described model. Hsu et al. [24] studied the effect of Nafion® impregnation of a dual electrode by cyclic voltammetry and a.c. impedance measurements. The dependence of the electrochemically active surface area (EAS) on Nafion® loading in the reactive layer is shown in Figure 5. The maximum in the EAS, as well as the minimum in the ohmic resistance of the cell, occurred at 0.67 mg Nafion® cm^{-2}. The performance of electrodes having the same support and a catalyst layer with and without PTFE were compared in Figure 6 [11]. A remarkable loss of cell performance occurred in the absence of PTFE in the electrode reactive layer. In dual layer electrodes, the presence of PTFE in the catalyst layer is essential to avoid flooding of the catalyst.

Inserting a diffusion layer between the support and the reactive layer improves electrode performance, particularly at high current density, as can be seen in

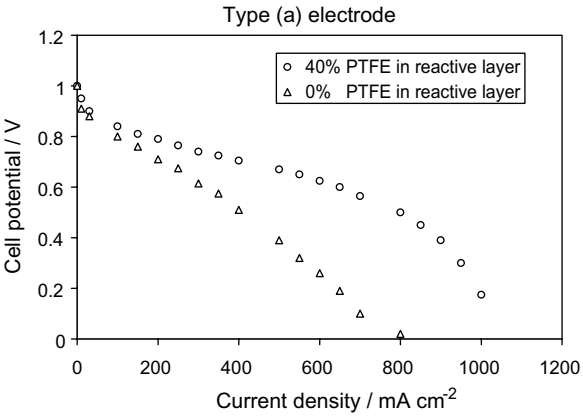

Fig. 6. Cell performance of PEFC type (a) electrodes with and without PTFE in reactive layer. Cell temperature 70 °C, in H_2/O_2 (2.5/3 bar) [11]. Substrate Toray with 30 wt % FEP; catalyst layer with Pt loading 0.5 mg cm^{-2} and Nafion® loading 0.9 mg cm^{-2}.

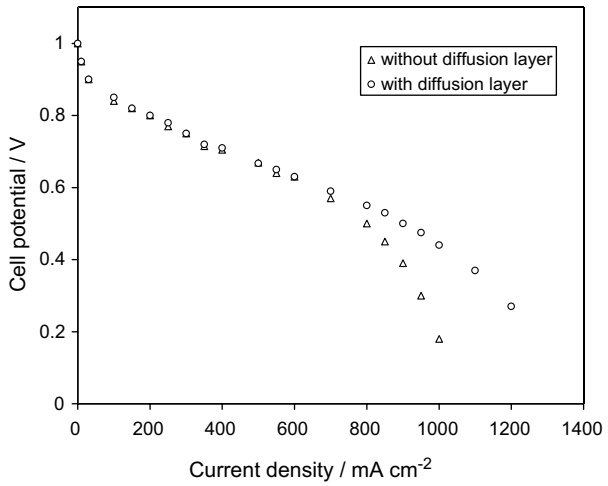

Fig. 7. Cell performance of PEFC electrodes with and without diffusion layer (with PTFE in the reactive layers of both electrodes). Cell temperature 70 °C. in H_2/air (2.5/3 bar) [11]. Substrate Kureha with 30 wt % FEP; catalyst layer with 40 wt % PTFE, Pt loading 0.5 mg cm^{-2} and Nafion® loading 0.9 mg cm^{-2}. Diffusion layer with 40 wt % PTFE and C loading 2 mg cm^{-2}.

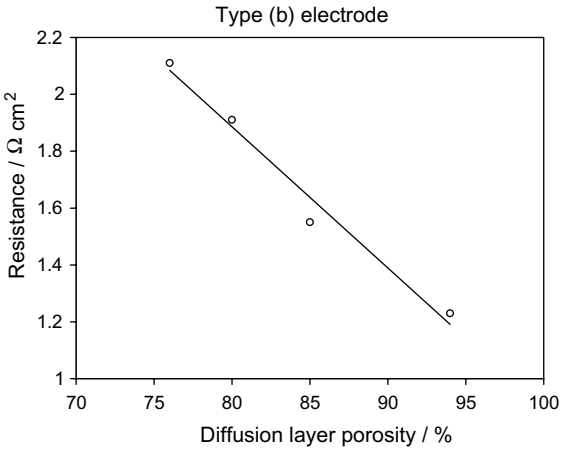

Fig. 8. Cell resistance *R* [26] against total porosity [25] of the diffusion layer of type (b) electrodes.

Figure 7 [11], where the performance in H_2/air operation of two electrodes having the same support and the same reactive layer are compared with and without an inserted diffusion layer. In the presence of a diffusion layer, a further improvement in electrode performance, as we will see later, can be obtained by using a thinner reactive layer without PTFE.

2.3. *Type (b) electrode*

As previously stated, experiments have demonstrated the advantage of placing a thin diffusion layer (made of fine carbon particles and PTFE) between the support and the catalyst layer. When using a diffusion layer, the water condensed in the support cannot readily penetrate into the catalyst layer.

2.3.1. *Diffusion layer*

The incorporation of PTFE serves two functions: binding the high surface carbon particles into a cohesive layer, and imparting a hydrophobic character to the layer. For the preparation of the diffusion layer, a homogeneous suspension is prepared by mixing the carbon with an appropriate amount of PTFE dispersion. This suspension is deposited onto the porous support. Then, the layer is dried and thermally treated in the same way as the reactive layer of dual electrodes. The pores of the diffusion layer must allow mass flow of the reactants (fuel and oxidant) to and of products (liquid water, at $T < 100$ °C) from the wetted pores of the active layer, where the electrochemical reactions take place. This requires a balance of hydrophilic (carbon surface) and hydrophobic (PTFE) pores. Antolini et al. [25] found that the polymer coats the pores with size lower than 1 μm (carbon inter-agglomerate pores), while the pores with size higher than 1 μm are not influenced by the presence of PTFE. Above 40 wt% PTFE, a further supply of polymer does not fill the pores, but increases the thickness of the layer. The presence of cracks, increasing in number and size with PTFE content, was also observed.

Giorgi et al. [26] carried out an out-of-cell study of the effect of the PTFE content in the diffusion layer on the performance of gas diffusion electrodes with a three layer structure. At high current density (diffusion control) the mass transport rate and, as a consequence, the cell performance increased with decreasing PTFE loading, due to the increase in total porosity. The possibility of electrode flooding was not taken into account in these out-of-cell measurements. Figure 8 shows the dependence of cell resistance *R* on total porosity. The term *R* represents the total contribution of the linear polarization components which include the charge transfer resistance of the hydrogen oxidation reaction (HOR), the resistance of the electrolyte in the cell and the linear diffusion terms due to diffusion of the gas phase in the diffusion layer and/or in the thin film [27]. As shown in Figure 8, in the absence of electrode flooding, the cell resistance decreases linearly with increasing electrode diffusion layer porosity. At low current density, the cell performance depends on the macroporosity of the diffusion layer and, as well as the macroporosity, passes through a minimum at 20 wt% PTFE. This behaviour was explained considering that a diffusion layer with a high macroporosity allows a higher effective catalytic area, because the spray deposited catalyst can penetrate into the larger pores of the diffusion layer, and, as a consequence, the triple contact zone Pt/ Nafion®/gas is increased. In recent work Chu et al. [28], using a half-cell model, showed that a fuel cell embedded with a diffusion layer with a larger averaged porosity consumes a greater amount of oxygen, so that a higher current density is generated and a better cell performance is obtained. According to the authors, the diffusion layer porosity has virtually no effect on the level of polarization when the current density is medium

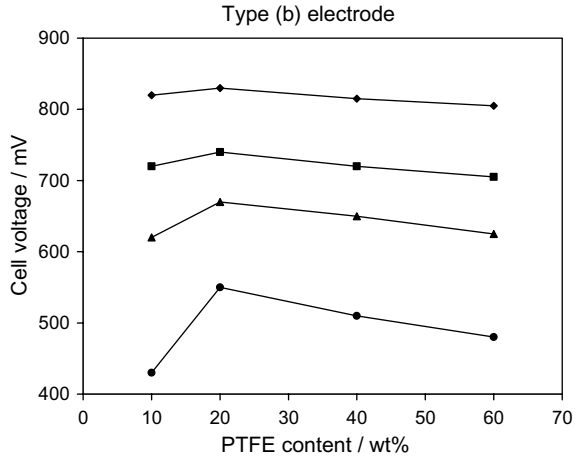

Fig. 9. Cell voltage against PTFE content in the diffusion layer at different current densities [29]. Cell temperature 70 °C, in H_2/air (2.5/3 bar). Current densities: (♦) 100; (■) 300; (▲) 500 and (●) 700 mA cm^{-2}.

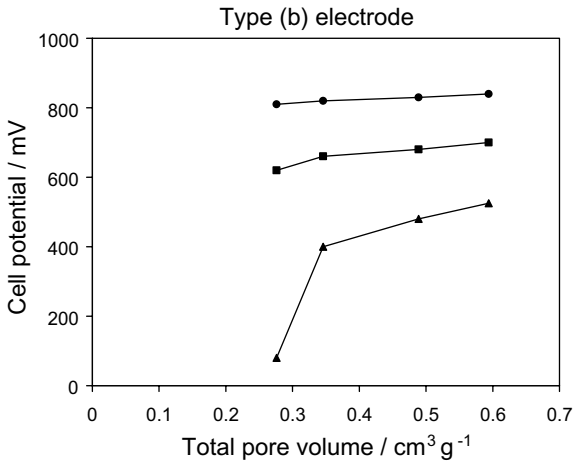

Fig. 10. Cell potential against total pore volume of the diffusion layer at several current densities [30]. Cell temperature 70 °C, in H_2/air (2.5/3 bar). Current densities: (●) 100; (■) 400 and (▲) 700 mA cm^{-2}.

or lower, but exerts a significant influence when the current density is high. This finding supports the scenario that the polarization at high current density corresponds mainly to mass transfer through the membrane/electrode assembly.

The optimum PTFE content in the diffusion layer was evaluated by Lufrano et al. [29] from the performance in H_2/O_2 and H_2/air of PEFCs with electrodes having a fluoropolymer content in the range 10–60 wt%. The same electrodes were used for anode and cathode. The best performance was obtained with a diffusion layer containing 20 wt% PTFE. The difference between the investigated electrodes was more evident in H_2/air operation, where the presence of a nitrogen blanket, together with product water, causes enhanced diffusion limitations due to the microporosity and/or to the hydrophobicity of the diffusion layer. The dependence of cell voltage at four different current densities on PTFE content of the diffusion layer is shown in Figure 9. At low current density (100 mA cm^{-2}) the effect is negligible, while at high current densities (500–700 mA cm^{-2}) the influence is more evident, showing a maximum at 20 wt% PTFE. The low performance of the 10 wt% PTFE electrode is probably due to the lower hydrophobicity, which is not enough to efficiently remove the water generated in the cell. Song et al. [9] have reported, using a.c. impedance measurements, that the optimal amount of PTFE in the diffusion layer was 30 wt%.

At a fixed content of PTFE of 20 wt%, Passalacqua et al. [30] determined the effect of the diffusion layer total pore volume on the cell performance at several current densities. The different pore volumes of the layer were obtained using several carbon blacks and graphite. The pore volume effect increases at high current density, as shown in Figure 10, where the cell potential at different current densities is plotted against the total pore volume of the diffusion layers. An increase in performance, more pronounced in the diffusion controlled region (> 400 mA cm^{-2}), was found when large pore volume layers were used. According to the authors, the presence of small secondary pores in these layers has a beneficial effect on the mass transport characteristics: this probably hinders the formation of large water drops, thus avoiding flooding and improving gas diffusion. Cells utilizing gas diffusion layers made with Acetylene Black carbon showed better performance compared with cells containing Vulcan XC-72R carbons. This result can be explained by the difference in porosity of the two carbons. Acetylene Black, with a lower pore volume in the 10–100 μm range, is thought to allow less liquid water to permeate into the diffusion layer. According to Neergat and Shukla [31], cells utilizing gas diffusion layers made with high surface area Ketjen Black carbon showed better performance compared with cells utilizing Vulcan XC-72 carbon or Acetylene Black carbon. By introducing macropores (around 50 to 100 μm in pore size) into the diffusion layer, Kong et al. [32] obtained a better cell performance. The macropores readily accumulate water in neighboring pores and form flow paths which are less resistive. So the macropores take in more water, while reducing the water saturation in the micropores. Thus the liquid and gas phases are effectively separated. Therefore, when large and straight pores are formed in the diffusion layer, liquid water can be preferentially transported through those pores, which reduces water saturation in smaller pores. The preferential water transport also makes it possible to confine droplet formation to prescribed locations.

Further to the hydrophobicity and the porosity, another important parameter is the size (thickness) of the diffusion layer. According to Song et al. [9], from a.c. impedance measurements the optimal amount of the diffusion layer turned out to be approximately 3.5 mg cm^{-2} with 30 wt% PTFE. Jordan et al. [33, 34] studied the effect of the carbon loading and carbon type of the diffusion layer with 10 wt% PTFE on PEFC

Table 2. Cell, hydrogen, and oxygen or air humidifier temperature found to give maximum power densities for various diffusion layer loadings at atmospheric pressure [34]

Diffusion layer Loading /mg cm^{-2}	Oxygen-fed cell			Power /W cm^{-2}	Air-fed cell			Power /W cm^{-2}
	H_2/°C	O_2/°C	cell/°C		H_2/°C	O_2/°C	cell/°C	
0.7	85	25	70	0.75	85	25	75	0.25
1.25	85	60	75	0.83	85	40	75	0.30
1.9	85	60	70	0.87	85	25	75	0.29
2.5	85	60	75	0.71	85	60	75	0.24

performance (same anode and cathode) in H_2/O_2 and H_2/air operation at atmospheric pressure. The maximum power densities derived from the cell potential–current density plots, along with optimum cell operating conditions, are shown in Table 2. As can be seen, the two intermediate loading diffusion layers performed better than either the lowest or highest diffusion layer loading. The difference in cell performance between oxygen and air is related to both the lower partial pressure of oxygen in air and the blanketing effect of nitrogen in air causing the diffusion effect to be different. Therefore, factors that improve gas diffusion may be more important for air than for oxygen fed cells. The optimum diffusion layer loading for each gas can be explained by diffusion limitations and/or water management problems at too high a loading. At low loadings, inadequate coverage of the diffusion layer carbon on the porous carbon paper could occur. This would lower the ability of the diffusion layer to support the catalyst layer in a homogeneous thin region. Interestingly, at the highest loading, the oxygen or air humidification temperature was highest indicating that, contrary to flooding, membrane hydration was difficult to achieve. Jordan et al. [33, 34] evaluated the effect of the sintering of the diffusion layer at 350 °C for 30 min on cell performance. The cell with the sintered diffusion layer, also performed better, at lower temperature, at high current density, with respect to the cell with the nonsintered diffusion layer operating at higher temperature, leading to the belief that sintering of the PTFE containing a diffusion layer replaces the function of higher cell temperature by managing water in the cell. According to the authors, the diffusion layer may not be homogeneous and probably contains regions that are not suitably hydrophobic and/or possess large pores that allow liquid water to pass into the gas diffusion layer. Liquid water in the diffusion layer would add an extra diffusion barrier – diffusion in the gas phase being faster than diffusion through a liquid. On these bases, the effect of sintering thus provides a more homogeneous covering of PTFE in the gas diffusion electrode, making the gas diffusion layer more hydrophobic.

As previously indicated, in many cases the same electrode type is used for both electrodes, although the optimal design for anode and cathode diffusion layer may be different. Some authors [31, 35, 36] prepared membrane/electrode assemblies (MEAs) using anodes and cathodes with different diffusion layers. Dissimilar results were obtained in oxygen fed cells. Moreira et al. [35] observed the best cell performance in H_2/O_2 operation with a combination of 10 and 30 wt% of PTFE, respectively, in the cathode and anode. Neergat and Shukla [31], instead, found that the cells with a hydrophilic diffusion layer on the anode and a hydrophobic diffusion layer on the cathode yield better performance both with oxygen and air as the oxidant. Besse et al. [36] evaluated the effect of PTFE content (in the range 25 to 50 wt%) in the cathode on cell performance, using an anode with 15 wt% PTFE. In H_2/O_2 operation, the cell performance was independent of PTFE content in the cathode, while in H_2/air operation the best performance was attained with the cathode containing 45 wt% PTFE. According to the authors, in the presence of humidified air, water transport has to be very fast to avoid electrode flooding. Water management is better with a high PTFE content in the cathode, a high water concentration gradient through the membrane and an increase in the electro-osmotic flow from the cathode to the anode.

2.3.2. *Catalyst layer*

As previously seen, using a diffusion layer, the presence of a hydrophobic agent in the reactive layer is not essential. Indeed, as shown in Figure 11, in contrast to type (a) electrodes, type (b) electrode without PTFE in the catalyst layer performed better than the same

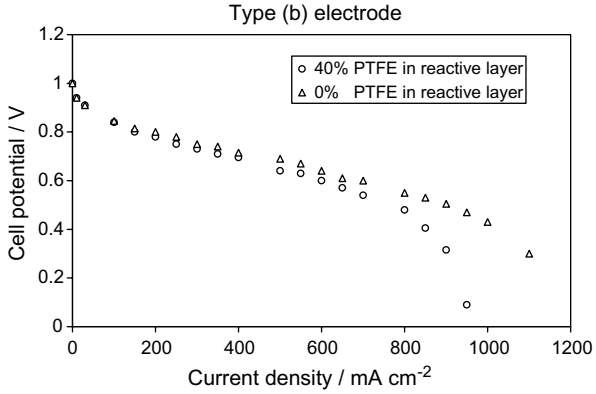

Fig. 11. Cell performance of type (b) electrodes with and without PTFE in reactive layer. T cell 70° C, in H_2/O_2 (2.5/3 bar) [11]. Substrate Kureha with 30 wt % FEP; diffusion layer with carbon loading 2 mg cm^{-2} and 40 wt % PTFE; catalyst layer with Pt loading 0.5 mg cm^{-2} and Nafion® loading 0.9 mg cm^{-2}.

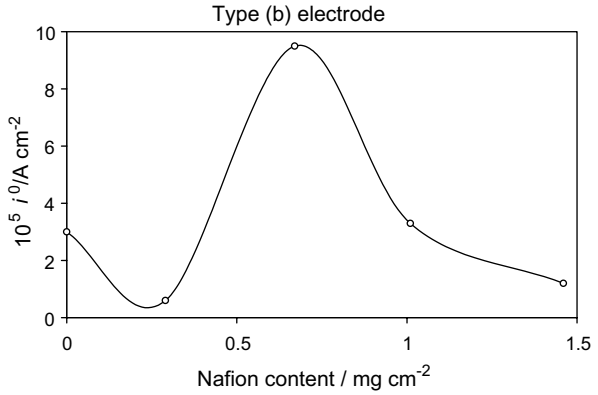

Fig. 12. Dependence of the exchange current density i_o on Nafion® content in the catalyst layer of type (b) electrodes [38].

electrode with PTFE in the reactive layer. Qi and Kaufman [37] prepared catalyst layers using various methods, with and without PTFE. One of the simplest methods was to mix supported catalysts with Nafion® solution and water without adding additional organic solvent. This method was not only simpler, safer and more economical, but also achieved better performance. The pore structure of the reactive layer has to allow the penetration of the electrolyte into the pores with the formation of a thin film covering the pores. This electrolyte film extends the three dimensional reaction zone and should be as thin as possible, to allow a short diffusion path for the reactant gases. By increasing the Nafion® concentration, the ionic conductivity is enhanced, but a too thick polymer layer inside the pores introduces mass transport limitations by retarding gas access to the active sites. According to Antolini et al. [38], the optimum Nafion® loading minimizes charge transfer resistance, ionic and gas transport limitations. They found that the exchange current density goes through a maximum value at 0.67 mg Nafion® cm^{-2}, as shown in Figure 12. In the absence of PTFE in the reactive layer (no subsequent thermal treatment is required), a method of preparation alternative to the impregnation method early described is to mix supported catalyst with Nafion® directly in the presence of glycerol [39, 40]. The purpose of adding glycerol is to form a mixture that is relatively viscous and holds the catalyst particles in suspension to minimize their agglomeration. The optimum Nafion® contents in the reactive layer from different sources are reported in Table 3. As can be seen, when the ionomer is introduced in the catalyst layer by impregnation, the optimum Nafion® content is lower than that introduced by placing it in the catalyst ink. There are two ways of explaining this behaviour. One is the difficulty for the Nafion® introduced by the impregnation to reach all catalyst particles, especially the inner Pt/C particles in the reactive layer. Another explanation is related to the following: when the Nafion® is introduced by impregnation, PTFE is always present in the reactive layer. Since both PTFE and Nafion® fill the pores of the catalyst, a lower amount of ionomer will cause mass transport problems. Finally, Yoon et al. [43] found that the use of a pore forming agent assists the transport of oxygen through the reactive layer.

2.4. *Type (c) electrode*

When carbon cloth is used as the support, the best electrode performance was obtained with the presence of two diffusion layers, one on the gas side and the other on the catalyst side of the substrate. As reported by Antolini et al. [44], to evaluate in detail the effect of gas side and catalyst side diffusion layer, two cathodes, one without the catalyst side diffusion layer, and the other without the gas side diffusion layer were tested, and their performances were compared with those of corresponding cathodes with two diffusion layers. Without the catalyst side diffusion layer, the catalyst ink goes within the carbon cloth, causing the absence of contact of the catalyst with the Nafion® membrane, so dramatically decreasing the cell performance. On the other hand, the performance of the cell without a gas side diffusion layer was the same at low current density, but lower at high current density than that of the cell with a cathode with two diffusion layers, having the same PTFE content in the catalyst side diffusion layer.

Generally, the performances of type (c) electrodes are higher than those of type (b) electrodes [45]. The performance of the cell with cathodes having both carbon paper and carbon cloth as support with Vulcan carbon in the diffusion layer, and carbon cloth with Shawinigan carbon in the diffusion layer are compared in Figure 13. The performances are reported at 85 °C for optimum H_2/O_2 pressure conditions for both carbon types. Both the electrodes with carbon cloth as the

Table 3. Optimum Nafion® loading (Nafion®/(Nafion® + Pt/C) in the catalyst layer from different sources

Electrode type	PTFE presence in the reactive layer	Nafion® introduction method	Optimum Nafion® /wt%	Reference
(a)	yes	impregnation	25	[24]
(a)	yes	impregnation	27	[23]
(a)	not	in the catalyst ink	33	[21]
(b)	not	in the catalyst ink	30	[37]
(b)	not	in the catalyst ink	33	[41]
(b)	not	in the catalyst ink	38	[38]
(c)	not	in the catalyst ink	35	[42]

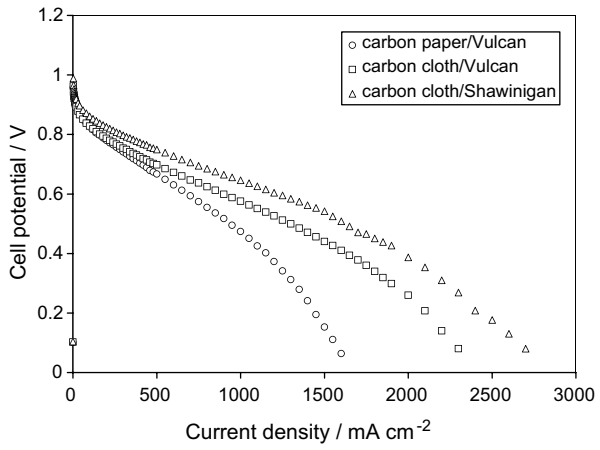

Fig. 13. Cell potential against current density plots for PEFCs at 85 °C [45]. The measurements were performed in H_2/O_2 at 2/2 atm for the electrodes with carbon paper or carbon cloth as support and Vulcan carbon in the diffusion layer and at 2/5 atm for the electrode with carbon cloth as support and Shawinigan carbon in the diffusion layer.

support performed better than those with carbon paper. The cell with Shawinigan carbon in the diffusion layer showed the best performance.

Paganin et al. [42] carried out electrochemical studies on type (c) electrodes with identical sublayers. MEAs were prepared using the same electrodes as anode and cathode. The best performance was obtained with electrodes formed from 20 wt% Pt/C, 0.4 mg Pt cm^{-2} and 1.1 mg Nafion® cm^{-2} in the catalyst layer, and 15 wt% PTFE in a diffusion layer of 50 μm thickness. Figure 14 shows the dependence of the cell resistance R on the thickness of the diffusion layer (Figure 12(a)) and on Nafion® content in the reactive layer (Figure 12(b)). Antolini et al. [44] compared the performance of PEFCs in H_2/air operation using cathodes with diffusion layers presenting different characteristics. The same anode with 15 wt% PTFE in both diffusion layers was used in all the cells. The best result was obtained using cathodes having PTFE content in the gas side diffusion layer higher than that in the catalyst side diffusion layer (30 wt% PTFE in the gas side and 15 wt% PTFE in the catalyst side diffusion layer). This behaviour was explained in terms of better water management within the cell. In further work the same authors [45] compared the performance of cathodes with Shawinigan and Vulcan carbons in the diffusion layer. The specific surface areas of Shawinigan and Vulcan carbons are 80 and 255 $m^2\ g^{-1}$, respectively. The study was always conducted using Vulcan carbon in the anode diffusion layer and the same Pt/C catalyst in the catalyst layers of the anode and cathode. The performance of PEFC using Shawinigan in both the diffusion layers of the cathode having carbon cloth as support was higher than that of the cell using Vulcan. The effect of the carbon type increased with increasing oxygen pressure. At an oxygen pressure of 3 atm, the presence of Shawinigan in the catalyst side diffusion layer decreases both E_o (negative effect on the cell performance) and R (positive effect on the cell performance). The electrocatalytic activity for ORR is slightly higher with Vulcan in the catalyst side diffusion layer. To optimize the cell performance at high pressures, the results suggest the use of cathodes with Vulcan carbon in the catalyst side and Shawinigan carbon in the gas side diffusion layers.

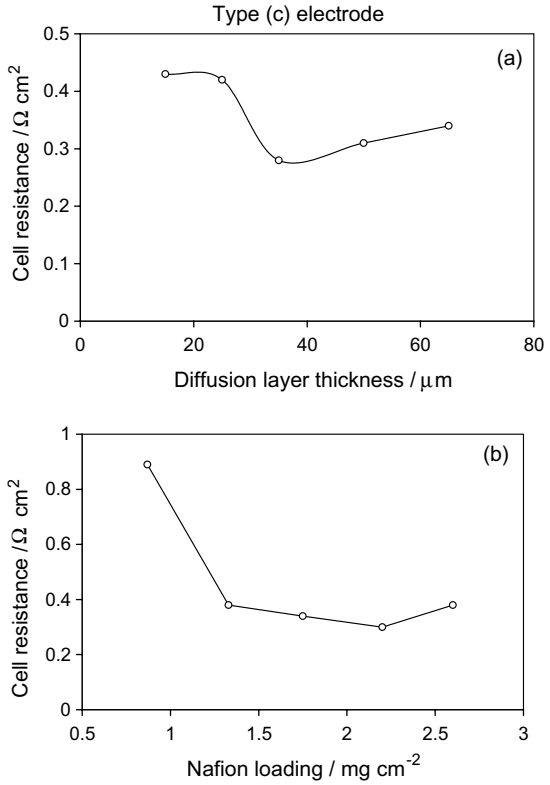

Fig. 14. Cell resistance R against diffusion layer thickness (a) and Nafion® content in the reactive layer (b) of type (c) electrodes [42].

2.5. *Preparation method*

Different techniques are used to deposit diffusion and catalyst layers. Table 4 shows some of these deposition techniques reported in the literature. For commercialization the spray technique is the most promising because a production line can be fully automated, therefore the electrode fabrication can be readily scaled up. Wilson and Gottesfeld [39] prepared electrodes of low platinum loading (about 0.1 mg cm^{-2}) by casting thin films without PTFE, with a thickness of a few μm, from a

Table 4. Some techniques for depositing diffusion and catalyst layers of PEFC electrodes

Reference	Diffusion layer	Catalyst layer
[16]	–	Screen-printing
[46]	–	Plating bath
[42]	Filtering	Brushing
[47]	Spraying	Spraying
[26]	Spraying	Spraying

suspension of Pt/C particles in solubilized Nafion® onto an inert support and subsequently by hot-pressing the dried film directly onto the membrane surface. Alternatively, they prepared the membrane/electrode structure by painting a suspension of the catalyst in solubilized Nafion® in the salt form Na^+ onto a ionomeric membrane also in the form Na^+ [40]. Then the layer was dried at 160–190 °C. A further improvement to increase the stability of the electrodes can be obtained by converting the Nafion® in a thermoplastic form (in the salt form tetrabutylammonium (TBA^+)) [48]. A conventional gas diffusion layer can then be attached to the thin reactive layer. The ohmic resistance of the membrane-electrode was 0.10 Ω cm^2 instead of the value of 0.12–0.15 Ω cm^2 using the conventional electrode [40]. Chun et al. [49] found that the performance of a direct coated thin film catalyst layer was higher than those of the conventional and transfer printing techniques. Conventional and thin film MEAs showed a performance of 350 and 650 mA cm^{-2} at 0.6 V, respectively.

3. CO tolerant anodes

To enhance the tolerance of reformed fuels, a remarkable improvement was made using Pt alloys, particularly PtRu, but also PtMo, PtSn, PtNi and PtCo. The PtRu loading in the catalyst layer determines the degree of CO-tolerance, and the optimal loading is also dependent on the fuel cell operation conditions such as current density, cell temperature and CO concentration. Higher current density, lower cell temperature and higher CO concentration require a higher PtRu loading [50]. Various types of mechanism have been proposed to explain the enhancement of H_2/CO electrooxidation on alloying Pt with Ru. Those most proposed are the bifunctional catalyst effect (promoted mechanism) and the modification of the electronic properties of the Pt (intrinsic mechanism).

(a) *Promoted mechanism*

According to Oetjen et al. [51] the electrocatalysis of H_2 in the presence of CO can be described by the competitive adsorption of hydrogen and carbon monoxide on platinum sites:

$$3\,Pt + H_2 + CO \rightarrow Pt - CO_{ads} + 2\,Pt - H_{ads} \qquad (1)$$

The reduction of cell performance is related to CO adsorption which blocks sites for electrooxidation of hydrogen. The possibility to eliminate CO adsorbed depends on the following reactions [52] :

$$Pt + H_2O \rightarrow Pt - OH_{ads} + H^+ + e^- \qquad (2a)$$

$$Ru + H_2O \rightarrow Ru - OH_{ads} + H^+ + e^- \qquad (2b)$$

$$Pt - CO_{ads} + Pt - OH_{ads} \rightarrow 2\,Pt + CO_2 + H^+ + e^- \qquad (3a)$$

$$Pt - CO_{ads} + Ru - OH_{ads} \rightarrow Ru + Pt + CO_2 + H^+ + e^- \qquad (3b)$$

The Reactions 2(b) and 3(b) occur at lower potentials than Reactions 2 and 3. The oxidation of the strongly adsorbed CO present in the fuel is facilitated in the presence of Ru by supplying oxygen atoms at an adjacent site at a lower potential than that accomplished by pure Pt. The bifunctional mechanism on PtRu alloys was theorized by measurements on a rotating disk electrode [53] and IR spectroscopy [54]. Previous work reported that the best activity for CO oxidation was found for a PtRu alloy having a bulk Pt:Ru atomic ratio of 1:1 [54–57]. The fact that Pt:Ru = 1:1 showed that the lowest CO oxidation potential supports the bifunctional mechanism according to Equation 3(b), where Ru adsorbs the oxygen-containing species and CO bind to Pt. CO adsorption is equally facile at Pt–Pt, Ru–Ru and Pt–Ru sites, but a reduced adsorption strength of OH on Pt–Ru pairs was suggested by Gasteiger et al. [53], who stated that for a composition of 50 at % PtRu the number of Pt–Ru sites is maximized.

(b) *Intrinsic mechanism*

The intrinsic mechanism postulates that the presence of Ru modifies H_2 and CO chemisorption properties, so as to reduces CO coverage with respect to H_2 oxidation sites [58]. This mechanism is based on electron donation/back donation which acts in the Pt-CO bond. The CO adsorption on Pt is stabilized by two simultaneous effects [59]: (i) electron transfer from the CO-filled 5σ molecular orbital to the empty dσ band of Pt; (ii) back-donation of electrons from the metal dπ orbital to the empty $2\pi^*$ antibonding orbital of CO.

The effect of alloying on Pt electronic structure was evaluated, to better understand the hydrogen and methanol oxidation mechanism. The modification of the Pt d band occupancy can be used to determine the degree of alloying. Watanabe and Motoo [60] found by Fourier transform infrared spectroscopy studies a higher frequency for the CO stretch on PtRu, implying a lower energy of absorption for CO on the alloy compared to pure Pt. To confirm this result, work by Krauza and Vielstich [61] indicated that the peak potential for the CO residue formation is shifted 70 mV in the negative direction on the alloy. According to Iwasita et al. [62], electronic effects on alloying can explain the lower energy of CO absorption. Goodenough and Manoharan [63] combined X-ray photoelectron spectroscopy, extended X-ray absorption fine structure (EXAFS) and electron spin resonance measurements on carbon supported PtRu, to conclude that synergistic catalytic effects result from an intra-alloy electron transfer from Ru to Pt. Pt X-ray absorption near edge structure spectroscopy (XANES), performed by McBreen and Mukerjee [64] on Pt, Pt/C and PtRu/C catalysts, indicated that alloying with Ru causes an electronic effect on the Pt. The calculated Pt d band vacancies in the double-layer region (0.54 V) were 0.397, compared

with a value of 0.329 for a Pt/C catalyst. So, alloying with Ru causes an increase in the number of Pt d band vacancies. In such a situation the synergistic mechanism of interaction of the Pt–CO bond looses its stabilizing effect. Ipo-electronic metals, such as Ru, Mo etc., produce a shift effect and charge redistribution, which strongly influences the CO adsorption phenomena. The same mechanism of CO tolerance in H_2 oxidation was proposed by Igarashi et al. [65] for PtFe, PtNi, PtCo and PtMo alloys, regardless of the composition.

From studies on both half and single cell polarization characteristics at several temperatures and CO partial pressures for Pt/C, PtSn/C and PtRu/C electrocatalysts, Lee et al. [66] inferred that both the oxidation of CO by the alloy catalysts and the change in the thermodynamics and the kinetics of the CO adsorption process, induced by the alloy, contribute to CO-tolerance.

Pozio et al. [59] from half-cell measurements in H_2SO_4 on E-TEK PtRu/C catalysts reported the optimum Pt:Ru value of 1:1. Antolini et al. [67] investigated PEFC performance using PtRu/C electrocatalysts by E-TEK with different Ru content. The cell voltage at a current density of 0.5 A cm^{-2} for anodes with various PtRu catalysts in different operating conditions is shown in Table 5 [67]. The best value was obtained for Pt:Ru catalyst with atomic ratio 1:1. To evaluate the net Ru effect, they normalized the voltage of the PtRu samples in CO operation with respect to the thickness effect, related to the different carbon contents of the catalyst layer. Figure 15 shows the normalized cell voltage against Ru content plot for PtRu anodes: at both 70 and 90 °C, by a three-order regression analysis of experimental values, a sigmoidal curve was obtained with a maximum of 63 at % Ru. Taking into account that, especially for high Ru contents, only part of the Ru present in the catalyst forms a face centered cubic (f.c.c.) PtRu alloy, this value is probably related to the maximum number of PtRu pairs. Camara et al. [68] prepared PtRu/C catalysts by a sulfide complex method and achieved the best CO-tolerance for 3:1 Pt:Ru alloy actual composition. These different values of the optimal catalyst composition can be related both to surface composition, depending on the preparation method of the catalyst, and to unalloyed Ru [69]. Recently, Qi and Kaufman [50] found that PtRu/C catalysts with same Pt:Ru atomic ratio 1:1 and same Pt–Ru crystallite size made by different manufacturers have different CO-tolerances under the same operating conditions. This

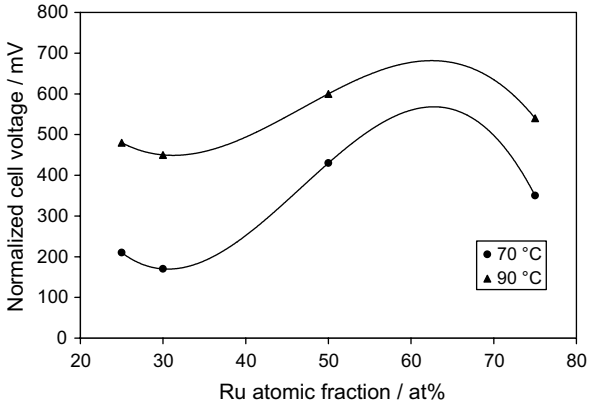

Fig. 15. Normalized cell voltage at 0.5 A cm^{-2} and different cell temperatures in H_2 + CO operation against Ru content of PtRu/C catalysts [67].

behaviour can also be attributed to the previously described features.

PtRu alloys and PtMo alloys have also been extensively studied [59, 70–72]. Gouérec et al. [70] found that unsupported PtMo with low Mo content (~5 at %) displays a similar performance in (H_2 + 100 ppm CO)/O_2 fuel cell tests to that by unsupported Pt:Ru with atomic ratio 1:1. Pozio et al. [59] studied carbon supported PtMo catalysts with nominal composition 3:1, 4:1 and 5:1. The electrode with PtMo/C with Pt:Mo atomic ratio 5:1 showed the best performance in H_2 + CO operation, comparable with that of PtRu/C catalyst with Pt:Ru 1:1. Grgur et al. [71] found that carbon supported PtMo catalysts with atomic ratio 3:1 and 4:1 have significantly better CO-tolerance in polymer electrolyte membrane fuel cells than PtRu alloy catalytst. Mukerjee et al. [72] found a two to three fold enhancement of CO-tolerance in PEFCs with PtMo/C as compared to the current state of the art PtRu/C electrocatalysts. The alloy composition was Pt:Mo in the atomic ratio 8.7:1.3 determined by both XRD and *in situ* EXAFS measurements. Rotating disc electrode measurements and cyclic voltammetry in a PEM fuel cell indicate that the oxidation of CO involves oxyhydroxides of Mo.

As well as having good CO tolerance, PtM alloys must have a high electrocatalytic activity for HOR. At present, the best CO tolerant catalyst (PtRu with atomic ratio 1:1) shows a decrease in catalytic activity of 25% compared to pure Pt. In the case of PtRu alloys, the

Table 5. Cell voltage (mV) at a current density of 0.5 A cm^{-2} for PtRu/C electrocatalysts with various Pt:Ru atomic ratio in different operating conditions [67]

Electrocatalyst	70 °C, H_2	70 °C, H_2 + CO	90 °C, H_2	90 °C, H_2 + CO
20% Pt	636	105	672	205
20% PtRu 3:1	630	201	657	476
20% PtRu 7:3	610	136	650	436
20% PtRu 1:1	592	413	621	557
20% PtRu 1:3	350	89	626	529
40% PtRu 1:1	649	415	674	611

charge transfer reaction is affected by the adsorption of oxygen-containing species which increases with increasing amount of Ru (positive effect). On the other hand, hydrogen adsorption increases with increasing number of neighbouring Pt–Pt, but the nearest Pt–Pt amount decreases with increasing Ru content in the alloy (negative effect). Catalysts with Pt:Ru atomic rato 1:1 seem to guarantee the best agreement of the two effects. But conflicting results concerning the optimal Pt:Ru atomic ratio for H_2 and H_2 + CO oxidation have been reported in work on phosphoric acid fuel cells. In the absence of CO (pure H_2) Ross et al. [73] found two maxima for limiting current values at 10 at % and 60 at % Ru. Analogously, in PEFCs Gamez et al. [74] observed two maxima in the exchange current for HOR at 25 at % and 75 at % Ru. In NaOH Ramesh et al. [75] observed a maximum for HOR at 60 at % Ru. Finally, Pozio et al. [59] found the best result for HOR at 50 at % Ru in H_2SO_4.

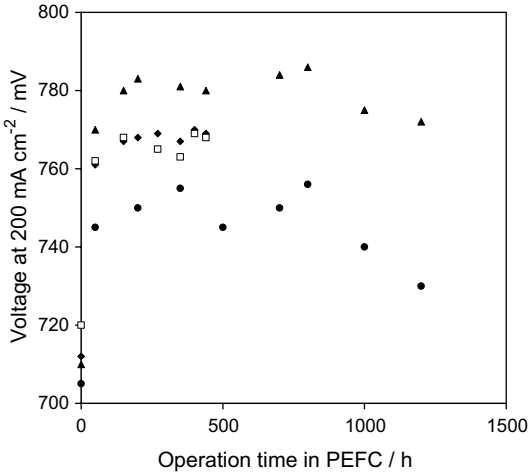

Fig. 16. Lifetime evaluation of carbon supported Pt and Pt alloy electrocatalysts for oxygen reduction in PEFCs [77]. Current density 200 mA cm^{-2}, cell temperature 50 °C, ambient pressure. (●) Pt; (□) PtCo; (♦) PtNi; PtCr (▲).

4. Cathodes with improved electrocatalysis of the oxygen reduction reaction

The presence of CO in the fuel is not a problem in phosphoric acid fuel cells, working at 200 °C, and, as a consequence, no studies have been carried out on CO-tolerant anodes in PAFCs. However, much work has been performed on platinum alloys with improved electrocatalysis for oxygen reduction in the PAFC environment. The effect of alloy formation on cathodic oxygen reduction in PAFCs was reviewed by Mukerjee [76]. The acid environment in PEFCs is different from that in PAFCs. The anions of the perfluorinated sulfonic acid polymer are only weakly adsorbed on Pt, in contrast to the phosphoric anions, which are strongly adsorbed. Furthermore, PEFCs operate at less than 100 °C, as compared with PAFCs, which operate at twice this temperature. A better stability of the catalyst in the PEFC environment is expected. Mukerjee and Srinivasan [77] evaluated the lifetime of carbon supported PtNi, PtCr and PtCo alloys in single PEFC at a constant current density of 200 mA cm^{-2}. Considering the excellent stability of the Dow membrane, the lifetime of a PEFC essentially depends on the catalyst stability. The cell potential at 200 mA cm^{-2}, monitored over a time period of 400–1200 h, is shown in Figure 16. There seems to be only a small deterioration in cell performance with PtCr/C and Pt/C cathodes over an operating time of 1200 h. The PtNi and PtCo electrodes, tested over a period of 400 h showed no loss of performance. Mukerjee et al. [77, 78] found an enhancement of electrocatalytic activity for ORR under PEFC conditions on carbon supported PtCo, PtCr, PtNi, PtMn and PtFe in the atomic ratio Pt:M = 3:1, as compared to that on Pt/C electrocatalyst. Some electrode kinetic parameters for oxygen reduction on Pt and Pt alloy electrocatalysts in PEFCs are shown in Table 6. A two to threefold activity enhancement in terms of geometric surface area of the electrode is indicated by the value of current density at 900 mV. A similar trend is observed for the values of exchange current density and the potential at 10 mA cm^{-2}. Plots of electrocatalytic activity ($i_{900\ mV}$) against the electronic (Pt d-band vacancies per atom, Figure 17(a)) and geometric (Pt–Pt bond distance, Figure 17(b)) parameters show a volcano curve behaviour. PtCr/C lies at the top of the curve, revealing the fact that, among the electrocatalysts investigated, it has the best combination of both the Pt d-band vacancies as well as the Pt–Pt bond distance.

According to Paganin [79] the performance in PEFCs of carbon supported PtCo, PtCr and PtV in the nominal atomic ratio Pt:M = 1:1 at an oxygen pressure of 1 atm, were lower than that of Pt/C.

Table 6. Electrode kinetic parameters for oxygen reduction on Pt and Pt alloy electrocatalysts in PEFCs at 95 °C and 5 atm pressure [78]

Electrocatalyst	E_o /mV	R /Ω cm^2	i_o /mA cm^{-2}	$i_{900\ mV}$ /mA cm^{-2}	$E_{10\ mA\ cm^{-2}}$ /mV
Pt/C	982	0.14	3.46	22.1	915
PtMn/C	995	0.10	6.26	40.1	945
PtCr/C	1005	0.09	7.15	83.8	951
PtFe/C	1001	0.10	6.94	50.4	948
PtCo/C	990	0.11	5.87	37.2	935
PtNi/C	988	0.11	4.86	26.4	924

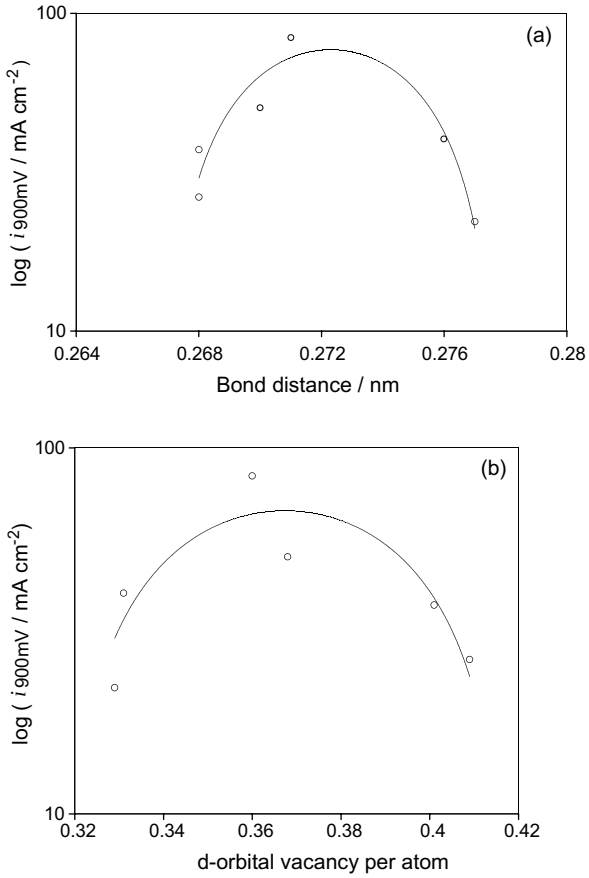

Fig. 17. Dependence of cathode performance (log $i_{900\,mV}$, mA cm^{-2}) of Pt and Pt alloy electrocatalysts in PEFCs on Pt–Pt bond distance (a) and d-orbital vacancy of Pt (b) [78].

Antolini et al. [80] investigated the electrocatalysis of the oxygen reduction reaction on carbon supported PtV catalyst with a Pt:V ratio of 1:1 at interfaces with a proton exchange membrane. At an oxygen pressure of 1 atm comparison of Pt/C and PtV/C catalysts in PEFC operation indicated a lower electrocatalytic activity in the presence of vanadium. At O_2 pressure higher than 2 atm, an enhanced electrocatalysis by PtV/C compared to Pt/C was achieved. This indicates a different electrocatalytic mechanism of the ORR for Pt/C and PtV/C.

Shim et al. [81] investigated the catalytic activity of Pt–WO_3/C and Pt–TiO_2/C catalysts in PEFCs by cyclic voltammetry and in-cell operation. Adsorption characteristics for oxygen on the platinum surface and performances for the catalysts at 80 °C were greatly influenced by added oxide content in the catalysts.

5. Conclusions

The loss of performance during fuel cell operation is due both to the presence of liquid water causing flooding of the catalyst layer and mass transport limitation, and to the platinum poisoning by the use of reformed fuels. These problems were overcome by the introduction of a diffusion layer between the support and the reactive layer, and the use of Pt alloy electrocatalysts in the preparation of CO tolerant anodes. In the first case, better water management was obtained by optimization of the diffusion layer, in terms of hydrophobic characteristics and porosity. These improvements lead to a change in electrode configuration from a two to a three layer structure, and to the use of anodes and cathodes with different chemical composition of both the diffusion and the catalyst layer.

References

1. P. Costamagna and S. Srinivasan, *J. Power Sources* **102** (2001) 242.
2. P. Costamagna and S. Srinivasan, *J. Power Sources* **102** (2001) 253.
3. I.D. Raistrick, *in* J.W. Van Zee, R.E. White, K. Kinoshita and H.S. Burney (Eds), Proceedings of the Symposium on 'Diaphragms, Separators and Ion Exchange Membranes', The Electrochemical Society, Pennington, NJ (1986), p. 172.
4. S. Srinivasan, E.A. Ticianelli, C.R. Derouin and A. Redondo, *J. Power Sources* **22** (1988) 359.
5. E.A. Ticianelli, C.R. Derouin, A. Redondo and S. Srinivasan, *J. Electrochem. Soc.* **135** (1988) 2209.
6. D. Bevers, M. Wohr, K. Yasuda and K. Oguro, *J. Appl. Electrochem.* **27** (1997) 1254.
7. D.M. Bernardi and M.W. Verbrugge, *J. Electrochem. Soc.* **139** (1992) 2477.
8. E. Passalacqua, F. Lufrano, G. Squadrito, A. Patti and L. Giorgi, *Electrochim. Acta* **43** (1998) 3665.
9. J-M. Song, S-Y. Cha and W-M. Lee, *J. Power Sources* **94** (2001) 78.
10. Z. Qi and A. Kaufman, *J. Power Sources* **109** (2002) 38.
11. E. Passalacqua, F. Lufrano, G. Squadrito and A. Patti, *in* 'Development of Low Pt Loading Electrodes', external report (CNR Messina, June 1996).
12. Z. Poltarzewski, P. Staiti, V. Alderucci, G. Maggio, N. Giordano and A. Fasulo, *J. Appl. Electrochem.* **22** (1992) 663.
13. P. Staiti, Z. Poltarewski, V. Alderucci and N. Giordano, *Int. J. Hydrogen Energy* **19** (1994) 254.
14. M. Uchida, Y. Aoyama, M. Tanabe, N. Yanagihara, N. Eda and A. Ohta, *J. Electrochem. Soc.* **142** (1995) 2572.
15. M. Watanabe, M. Tomokawa and S. Motoo, *J. Electroanal. Chem.* **195** (1985) 81.
16. N. Giordano, E. Passalacqua, V. Alderucci, P. Staiti, L. Pino, H. Mirzaian, E.J. Taylor and G. Wilemski, *Electrochim. Acta* **36** (1991) 1049.
17. T. Maoka, *Electrochim. Acta* **33** (1988) 379.
18. J.H. Nam and M. Kaviany, submitted to *Int. J. Heat Mass Transf.*
19. X. Cheng, B. Yi, M. Han, J. Zhang, Y. Qiao and J. Yu, *J. Power Sources* **79** (1999) 75.
20. A.S. Aricò, V. Antonucci, V. Alderucci, E. Modica and N. Giordano, *J. Appl. Electrochem.* **23** (1993) 1107.
21. M. Uchida, Y. Aoyama, N. Eda and A. Ohta, *J. Electrochem. Soc.* **142** (1995) 4143.
22. S.J. Lee, S. Mukerjee, J. McBreen, Y.W. Rho, Y.T. Kho and T.H. Lee, *Electrochim. Acta* **43** (1998) 3693.
23. Z. Poltarewski, P. Staiti, V. Alderucci, W. Wieczarek and N. Giordano, *J. Electrochem. Soc.* **139** (1992) 761.
24. Y-S. Hsu, C-S. Hsu and Y-C. Cheng, *in* Proceedings of the 3rd International Fuel Cell Conference. Nagoya, Japan (1999), p. 503.
25. E. Antolini, A. Pozio, L. Giorgi and E. Passalacqua, *J. Mater. Sci.* **33** (1998) 1837.
26. L. Giorgi, E. Antolini, A. Pozio and E. Passalacqua, *Electrochim. Acta* **43** (1998) 3675.
27. Y.W. Rho and S. Srinivasan, *J. Electrochem. Soc.* **141** (1994) 2089.
28. H-S. Chu, C. Yeh and F. Chen, *J. Power Sources*, in press.
29. F. Lufrano, E. Passalacqua, G. Squadrito, A. Patti and L. Giorgi, *J. Appl. Electrochem.* **29** (1999) 445.

30. E. Passalacqua, G. Squadrito, F. Lufrano, A. Patti and L. Giorgi, *J. Appl. Electrochem.* **31** (2001) 449.
31. M. Neergat and A.K. Shukla, *J. Power Sources* **104** (2002) 289.
32. C-S. Kong, D-Y. Kim, H-K. Lee, Y-G. Shul and T-H. Lee, *J. Power Sources* **108** (2002) 185.
33. L.R. Jordan, A.K. Shukla, T. Behrsing, N.R. Avery, B.C. Muddle and M. Forsyth, *J. Appl. Electrochem.* **30** (2000) 641.
34. L.R. Jordan, A.K. Shukla, T, Behrsing, N.R. Avery, B.C. Muddle and M. Forsyth, *J. Power Sources* **86** (2000) 250.
35. J. Moreira, A.L. Ocampo, P.J. Sebastian, M.A. Smit, M.D. Salazar, P. del Angel, J.A. Montoya, R. Perez and L. Martinez, *Int. J. Hydrogen Energy* **28** (2003) 625.
36. S. Besse, G. Bronoel and J.F. Fauvarque, *in* 'Resumé des Journées d'Etude Piles à Combustible'. (Paris, 1999) p. 2102.
37. Z. Qi and A. Kaufman, *J. Power Sources* **113** (2003) 37.
38. E. Antolini, L. Giorgi, A. Pozio and E. Passalacqua, *J. Power Sources* **77** (1999) 136.
39. M.S. Wilson and S. Gottesfeld, *J. Appl. Electrochem.* **22** (1992) 1.
40. M.S. Wilson and S. Gottesfeld, *J. Electrochem. Soc.* **139** (1992) L28.
41. E. Passalacqua, F. Lufrano, G. Squadrito, A. Patti and L. Giorgi, *Electrochim. Acta* **46** (2001) 799.
42. V.A. Paganin, E.A. Ticianelli and E.R. Gonzalez, *J. Appl. Electrochem.* **26** (1996) 297.
43. Y-G. Yoon, G-G. Park, T-H. Yang, J-N. Han, W-Y. Lee and C-S. Kim, *Int. J. Hydrogen Energy* **28** (2003) 657.
44. E. Antolini, R.R. Passos and E.A. Ticianelli, *J. Appl. Electrochem.* **32** (2002) 383.
45. E. Antolini, R.R. Passos and E.A. Ticianelli, *J. Power Sources* **109** (2002) 477.
46. E.J. Taylor, E.B. Anderson and N.R.K. Vilambi, *J. Electrochem. Soc.* **139** (1992) L45.
47. G.S. Kumar, M. Raja and S. Parthasarathy, *Electrochim. Acta* **40** (1995) 285.
48. M.S. Wilson, J.A. Valerio and S. Gottesfeld, *Electrochim. Acta* **40** (1995) 355.
49. Y.G. Chun, C.S. Kim, D.H. Peck and D.R. Shin, *J. Power Sources* **71** (1998) 174.
50. Z. Qi and A. Kaufman, *J. Power Sources* **113** (2003) 115.
51. H.F. Oetjen, V.M. Schmidt, U. Stimming and F. Trila, *J. Electrochem. Soc.* **143** (1996) 3838.
52. A. Kabbabi, R. Faure, R. Durand, B. Beden, F. Hahn, J.M. Leger and C. Lamy, *J. Electroanal. Chem.* **444** (1998) 41.
53. H.A. Gasteiger, N.M. Markovic, P.N. Ross and E.J. Cairns, *J. Phys. Chem.* **98** (1994) 617.
54. V.M. Schmidt, R. Ianniello, H.F. Oetjen and H. Reger, *in* S. Gottesfeld, G. Halpert and A. Landgrebe (Eds), 'Proton Conducting Membrane Fuel Cells I', The Electrochemical Society Proceedings Series. Pennington, NJ (1995), p.1.
55. T. Iwasita, R. Dalbeck, E. Pastor and X. Xia, *Electrochim. Acta* **11/12** (1994) 1817.
56. H.A. Gasteiger, N.M. Markovic, P.N. Ross and E.J. Cairns, *Electrochim. Acta* **11/12** (1994) 1825.
57. R. Ianniello, V.M. Schmidt, U. Stimming, J. Stumper and A. Wallau, *Electrochim. Acta* **11/12** (1994) 1863.
58. P. Wolohan, P.C.H. Mitchell, D. Thompsett and S.J. Cooper, *J. Mol. Catal. A* **119** (1997) 223.
59. A. Pozio, L. Giorgi, E. Antolini and E. Passalacqua, *Electrochim. Acta* **46** (2000) 555.
60. M. Watanabe and S. Motoo, *J. Electroanal. Chem.* **60** (1975) 275.
61. M. Krauza and W. Vielstich, *J. Electroanal. Chem.* **379** (1994) 307.
62. T. Iwasita, F.C. Nart and W. Vielstich, *Ber. Bunsengen. Phys. Chem.* **94** (1990) 1030.
63. J.B. Goodenough, R. Manoharan, A.K. Shukla and K.V. Ramesh, *Chem. Mater.* **1** (1989) 391.
64. J. McBreen and S. Mukerjee, *J. Electrochem. Soc.* **142** (1995) 3399.
65. H. Igarashi, T. Fujino, Y. Zhu, H. Uchida and M. Watanabe, *Phys. Chem. Chem. Phys.* **3** (2001) 306.
66. S.J. Lee, S. Mukerjee, E.A. Ticianelli and J. McBreen, *Electrochim. Acta* **44** (1999) 3283.
67. E. Antolini, L. Giorgi, F. Cardellini and E. Passalacqua, *J. Solid State Electrochem.* **5** (2001) 131.
68. G.A. Camara, M.J. Giz, V.A. Paganin and E.A. Ticianelli, *J. Electroanal. Chem.* **537** (2002) 21.
69. E. Antolini, *Mater. Chem. Phys.* **78** (2003) 563.
70. P. Gouérec, M.C. Denis, D. Guay, J.P. Dodelet and R. Schulz, *J. Electrochem. Soc.* **147** (2000) 3989.
71. B.N. Grgur, N.M. Markovic and P.N. Ross, *J. Electrochem. Soc.* **146** (1999) 1613.
72. S. Mukerjee, S.J. Lee, E.A. Ticianelli, J. McBreen, B.N. Grgur, N.M. Markovic, P.N. Ross, J.R. Giallombardo and E.S. De Castro, *Electrochem. Solid State Lett.* **2** (1999) 12.
73. P.N. Ross, K. Kinoshita, A.J. Scarpellino and P. Stonehart, *J. Electroanal. Chem.* **63** (1975) 97.
74. A. Gamez, D. Richard and P. Gallezot, *in* 'Resumé des Journées d'Etude Piles à Combustible' (Paris, 1999), p. 401.
75. K.V. Ramesh, P.R. Sarode, S. Vasudevan and A.K. Shukla, *J. Electroanal. Chem.* **223** (1987) 91.
76. S. Mukerjee, *J. Appl. Electrochem.* **23** (1990) 537.
77. S. Mukerjee and S. Srinivasan, *J. Electroanal. Chem.* **357** (1993) 201.
78. S. Mukerjee, S. Srinivasan, M.P. Soriaga and J. McBreen, *J. Electrochem. Soc.* **142** (1995) 1409.
79. V.A. Paganin, PhD thesis, S. Paulo, Brazil (1996).
80. E. Antolini, R.R. Passos and E.A. Ticianelli, *Electrochim. Acta* **48** (2002) 263.
81. J. Shim, C-R. Lee, H-K. Lee, J.S. Lee and E.J. Cairns, *J. Power Sources* **102** (2001) 172.